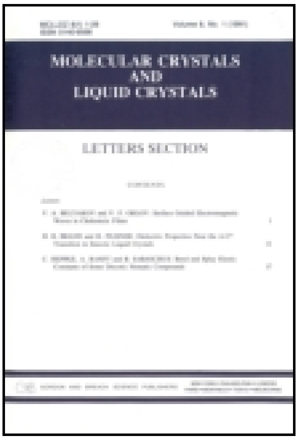

Molecular Crystals and Liquid Crystals
Publication details, including instructions for authors and subscription information:
http://www.tandfonline.com/loi/gmcl20

Analysis of Weak and Strong Discharge Characteristics for Fast Address Discharge in Microplasma Cells

Hyung Dal Park [a], Jae Hyun Kim [b], Heung-Sik Tae [b] & Bo-Sung Kim [c]

[a] Radiation Instrumentation Research Division, Korea Atomic Energy Research Institute, Daejeon, 305-353, Korea

[b] School of Electronics Engineering, College of IT Engineering, Kyungpook National University, Daegu, 702-701, Korea

[c] Display Nanomaterials Institute, Kyungpook National University, Daegu, 702-701, Korea

Published online: 08 Jan 2014.

Mol. Cryst. Liq. Cryst., Vol. 585: pp. 25–33, 2013

ISSN: 1542-1406 print/1563-5287 online
DOI: 10.1080/15421406.2013.852775

Analysis of Weak and Strong Discharge Characteristics for Fast Address Discharge in Microplasma Cells

HYUNG DAL PARK,[1] JAE HYUN KIM,[2] HEUNG-SIK TAE,[2,*] AND BO-SUNG KIM[3]

[1]Radiation Instrumentation Research Division, Korea Atomic Energy Research Institute, Daejeon 305-353, Korea
[2]School of Electronics Engineering, College of IT Engineering, Kyungpook National University, Daegu 702-701, Korea
[3]Display Nanomaterials Institute, Kyungpook National University, Daegu 702-701, Korea

In this paper, the voltage level of the negative falling ramp in the reset waveform is lower, the accumulated wall charges during the ramp-up period are more erased between A-Y electrodes, thus, reducing the number of wall charges prior to address discharge. In particular, the measured V_t closed-curves and the weak and strong discharge characteristics corresponding IR emission profiles show that fewer wall charges prior to an address discharge induce a decrease in the statistical time lag during the address period. The discharge transient contours of simultaneous discharges are changed by the wall voltage states after reset discharge, thereby influencing the statistical discharge time lag of the address discharge for the stable drive, thereby resulting in stable and fast addressing.

Keywords Fast address discharge; microplasma cells; V_t closed-curve; weak and strong discharge

Introduction

This paper provides the modified reset waveform for driving the stable and high speed address. The wall charge supplied from the reset period is an important factor in achieving fast and stable discharge characteristics during an address period. As the voltage level of the negative falling ramp in the reset waveform is lower, the accumulated wall charges during the ramp-up period are more erased between A-Y electrodes, thus reducing the amounts of wall charges prior to address discharge. In particular, the measured V_t closed-curves and the weak and strong discharge characteristics corresponding IR emission profiles show that fewer wall charges prior to an address discharge induce a decrease in the statistical time lag in the address period. The discharge transient contours of the simultaneous discharges are changed by the wall voltage states after reset discharge, thereby influencing the statistical

*Address correspondence to Prof. Heung-Sik Tae, School of Electronics Engineering, College of IT Engineering, Kyungpook National University Sangyuk-dong, Buk-gu, Daegu 702-701, Korea (KOR). Tel.: (+82)53-950-6563; Fax: (+82)53-950-5505. E-mail: hstae@ee.knu.ac.kr

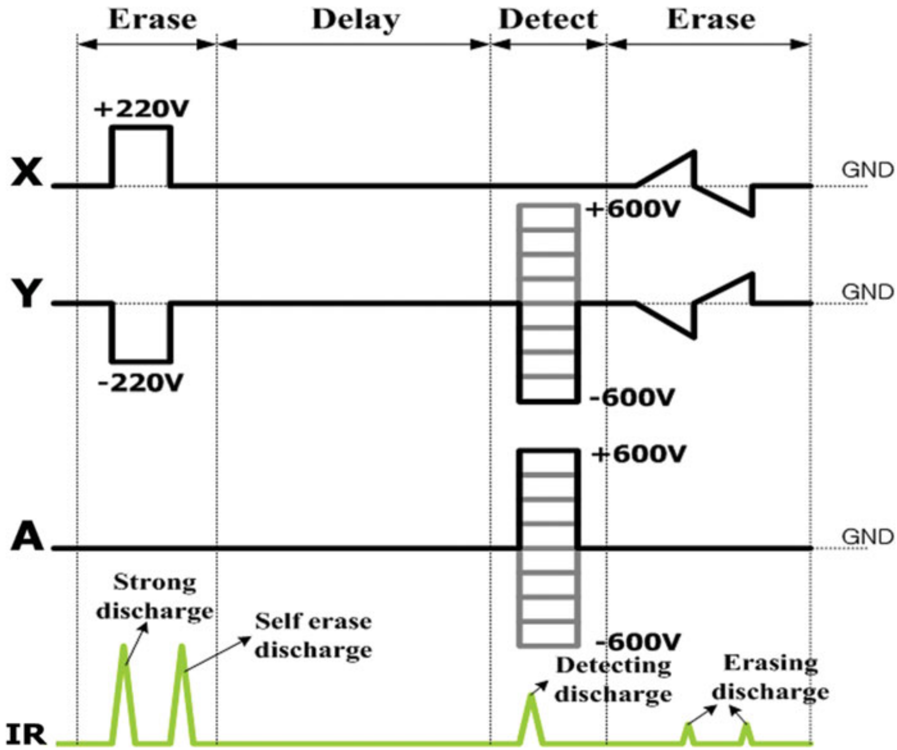

Figure 1. Driving waveform for measuring V_t closed-curves and discharge transient contours in case study.

discharge time lag of the address discharge for the stable drive, thereby resulting in stable and fast addressing.

Experimental Setup

The test panel used in this work was a commercial 50-in full HD AC-PDP with a box-type barrier rib. The gas mixture and pressure of the test panel were Ne-He-Xe (11%) and 420 Torr, respectively. The detailed specifications are listed in Table 1.

Table 1. Specifications of 50-in. Full HD Test Panel Employed in This Study

Front panel		Rear panel	
ITO width	220 μm	Barrier rib width	80 μm
ITO gap	70 μm	Barrier rib height	120 μm
Bus width	60 μm	Address width	90 μm
Cell pitch		576 μm	
Gas pressure		420 Torr	
Gas chemistry		Ne-He-Xe (11%)	
Barrier rib type		Closed rib	

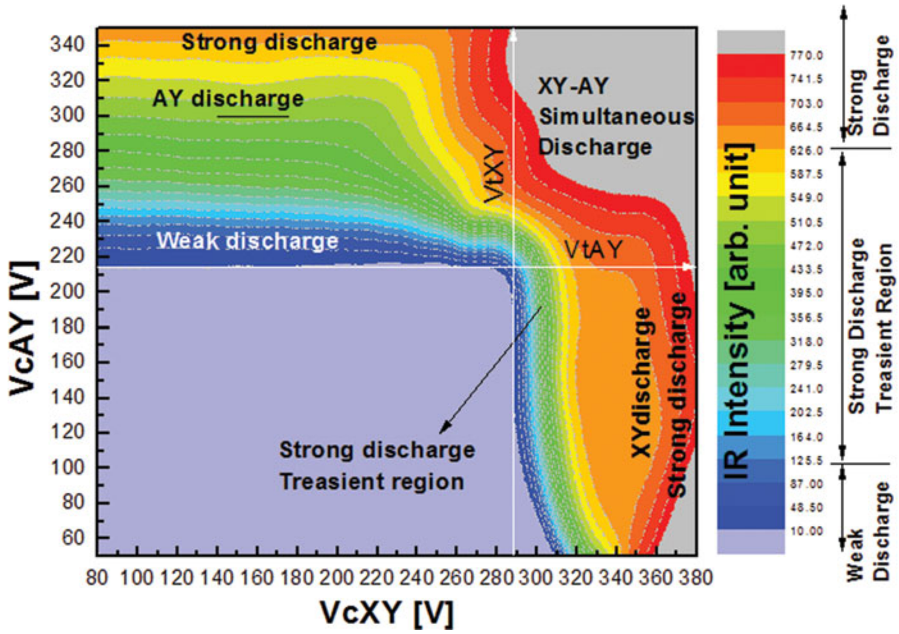

Figure 2. V_t closed-curves and discharge transient contour without initial wall voltage ($V_w = 0$) on test panel.

Figure 1 shows the driving waveform for measuring V_t closed-curves and discharge transient contour without initial wall voltage. A square-type waveform with a high voltage difference between the X-Y electrodes was applied to produce a strong discharge, thus completely eliminating the wall charge by inducing the ensuing strong self-erasing discharge. In addition, to exclude the priming effect, a detecting pulse was applied after 200 μs [1]. The discharge transient contours were measured by the same IR intensity according to the detecting pulse voltage during the detect period [2,3].

Table 2. Firing Voltages Measured From Cell in This Study

Sides	Firing voltage
MgO Cathode	
V_{tXY}	281 V
V_{tAY}	208V
V_{tAX}	192 V
V_{tYX}	280 V
Phosphor Cathode	
V_{tYA}	293 V
V_{tXA}	305 V

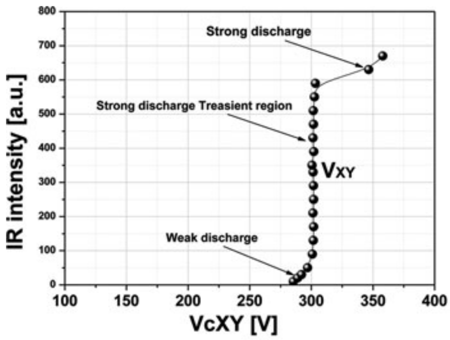

(a) XY discharge region
[cathode (Y): MgO, anode (X): MgO]

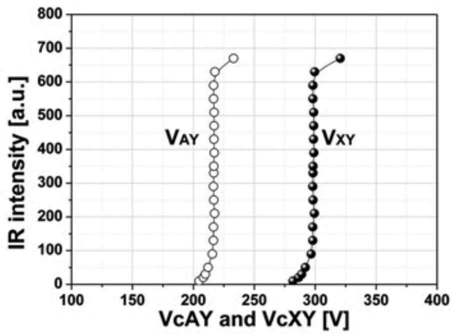

(b) XY-AY simultaneous discharge region
[cathode: MgO (Y), anode: MgO and phosphor (X, A)]

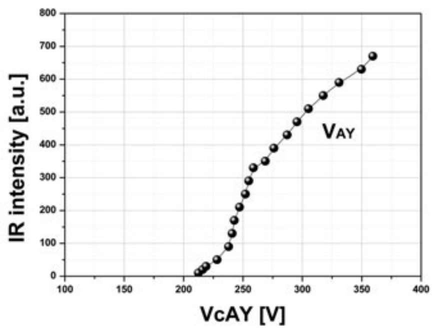

(c) AY discharge region
[cathode (Y): MgO, anode: phosphor (A)]

Figure 3. IR intensity by increasing applied voltage relative to V_t closed-curve and discharge transient contour without initial wall voltage ($V_W = 0$) in Fig. 2.

Result and Discussions

1. Weak and Strong Discharge Characteristics in Micro-Discharge Cells

Figure 2 shows the V_t closed-curves and the discharge transient contour at the same infrared intensity without the initial wall voltage on the test panel [4]. Figure 2 shows the quadrant I region of the measured V_t closed-curve and discharge transient contour at the same infrared intensity without the initial wall voltage on the test panel [5]. As shown in Fig. 2, the quadrant I region of V_t closed-curve can be divided into the following three discharge regions: (a) XY discharge region, (b) XY-AY simultaneous discharge region, and (c) AY discharge region. In each discharge region, there are three separate discharge modes, namely, the weak discharge region, strong discharge transient region, and strong discharge regions. These are shown in relation to the applied voltage on the cell voltage plane in three electrodes PDP without initial wall voltage. Table 2 shows the firing voltage of each discharge mode at the test panel.

Figure 3 shows the IR intensity in relation to increasing applied voltage relative to the V_t closed-curve and discharge transient contour without initial wall voltage ($V_W = 0$) in Fig. 2. As shown in Fig. 3, the IR emissions separate into three regions, namely, weak discharge, strong discharge transient region, and strong discharge region. Figures 3(a) and (b) show

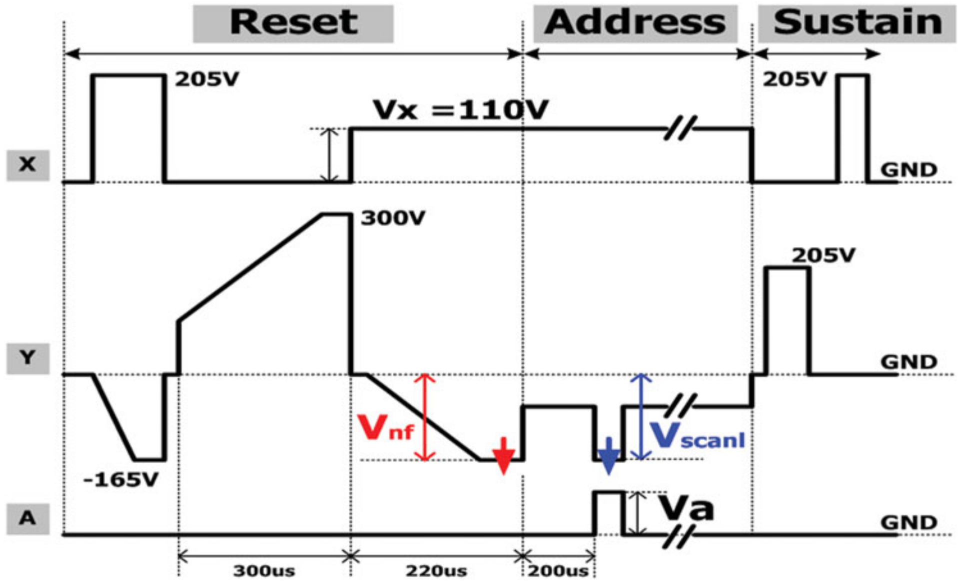

Figure 4. Driving waveform for improving address discharge delay time in case study.

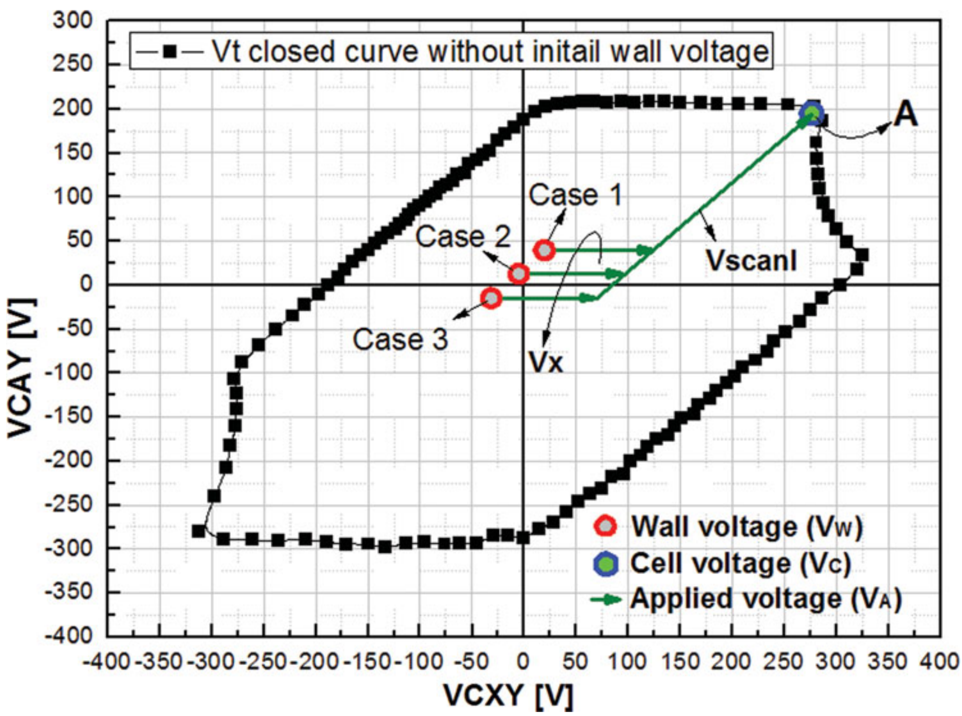

Figure 5. Cell voltage point ($V_C = V_W + V_A$) before address discharge, various wall voltage points (V_W) after reset discharge, and applied voltage vector (V_A) during address period on cell voltage plane in this study.

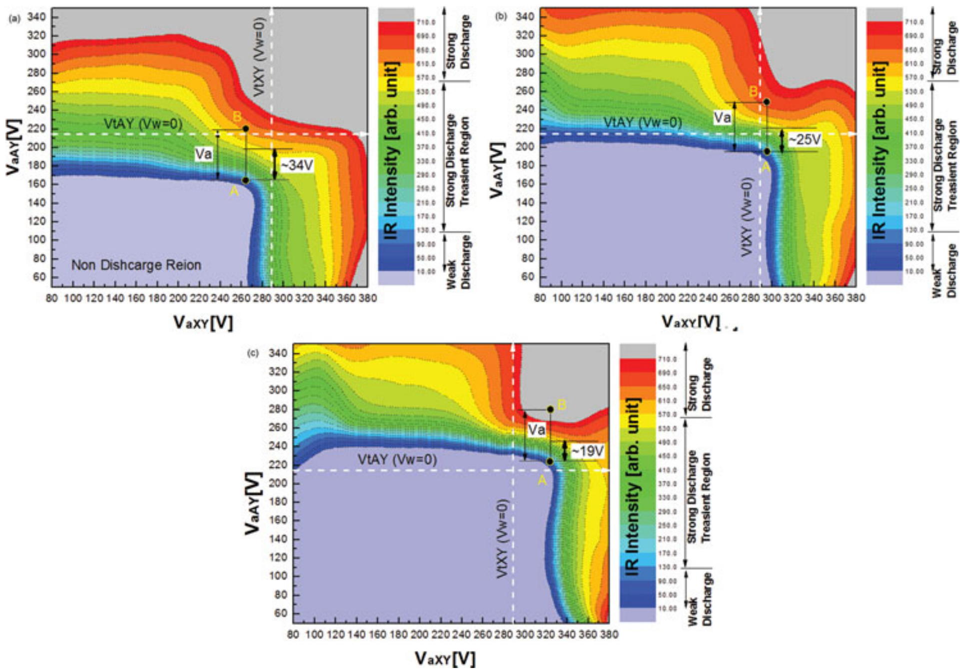

Figure 6. V_t closed-curves and discharge transient contour after reset discharge adopting various driving waveform of Fig. 5 and Table 3, respectively.

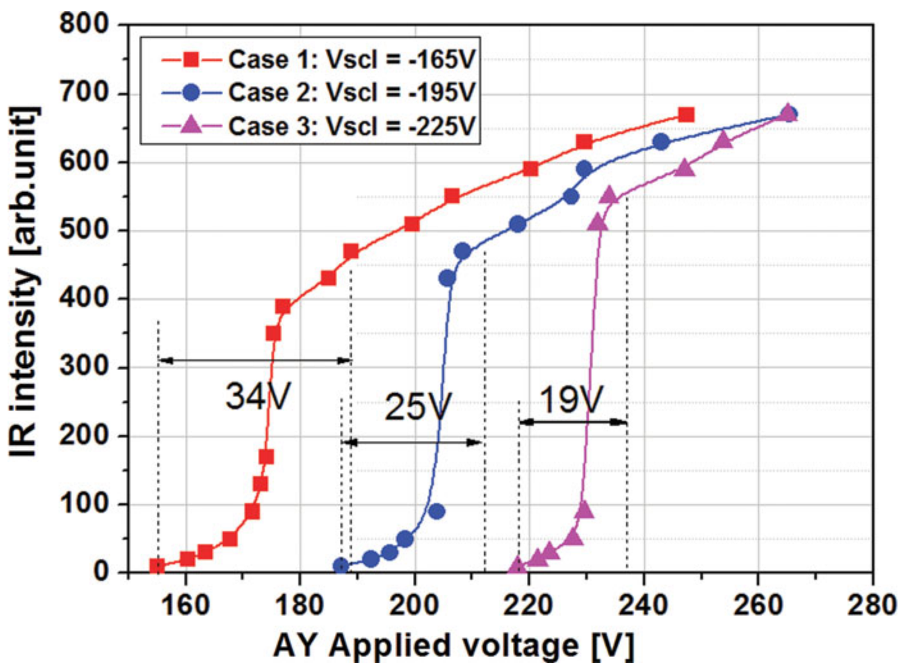

Figure 7. IR intensity by A-Y applied voltage relative to measured V_t closed-curve and discharge transient contour in Fig. 8.

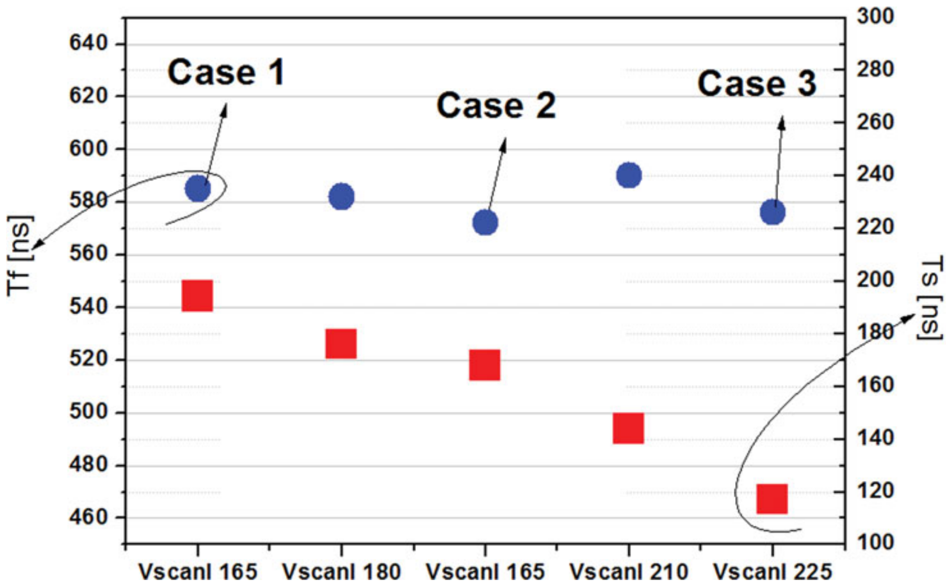

Figure 8. Address discharge delay time lags adopting various V_{scanl} levels.

the X-Y discharge and XY-AY simultaneous discharge regions. The IR intensities of the strong discharge transient region are dramatically increased by changing the small applied voltage. However, as shown in Fig. 3(c) of A-Y discharge region, the IR intensity of the strong discharge transient region is slowly increased by an increase in the applied voltage.

2. *Weak and Strong Discharge Characteristics by Wall Voltage States in Micro-Discharge Cells*

Figure 4 shows the driving waveform for improving the address discharge delay time in this study. Table 3 shows the various voltages used in case studies and voltage levels, V_{nf} and V_{scanl}, for the three cases. Different wall voltage conditions prior to an address discharge result in different applied voltage conditions to produce an address discharge: $V_{scanl} = -165$ V for case 1, $V_{scanl} = -195$V for case 2, $V_{scanl} = -225$ V for case 3, while V_S, V_X, and V_a are fixed at 205 V, 110 V, and 55 V, respectively.

Table 3. Various voltages used in case study and voltage level

Cases		V_{nf}	V_{scanl}
Case 1		−145 V	−165 V
Case 2		−175 V	−195 V
Case 3		−205 V	−225 V
		Voltage level	
V_S	205 V	V_a	55 V
V_X	110 V		

Table 4. Related address discharge delay time adopting various cases

Cases	Case 1	Case 2	Case 3
Tf [ns]	585	572	576
Ts [ns]	194	168	117
Td [= Tf + Ts] [ns]	779	740	693

Figure 5 shows the cell voltage point ($V_C = V_W + V_A$) before address discharge, various wall voltage points (V_W) after reset discharge, and the applied voltage vector (V_A) during the address period on the cell voltage plane in this study [6]. As seen in case 3 of Fig. 5, the wall voltage point is moved to the left and downward from case 1 to case 3. This means that the wall charges are more erased between A and Y electrodes. Also, the cell voltage, V_C, between the X, Y, and A electrodes is a sum of the wall voltage and the applied voltage, $V_W + V_A$ ($= V_X + V_{scanl}$). For cases 1, 2, and 3, the detailed voltage values are listed in Table 3. As shown in Fig. 5, for all cases, the cell voltages are the same at point A before the applied address voltage (V_a).

Figure 6 shows the V_t closed-curves and discharge transient contour after reset discharge adoption of various driving waveforms of Fig. 4 and Table 3, respectively. In case 1 of Figs. 6(a), the applied voltage for strong address discharge is needed by about 34 V from weak discharge to strong discharge region. The applied voltage between X-Y electrodes is 275 V [V_{aXY} (case 1) $<$ $V_{tXY} = 281$ V (VW = 0)] during the address period. However, in cases 2 and 3 of Figs. 6(b) and (c), the applied voltages for strong address discharge are needed by about 25 V and 19 V, respectively. The applied voltages between X-Y electrodes are 305 V and 335 V [V_{aXY} (case 2 and 3) $>$ $V_{tXY} = 281$ V ($V_W = 0$)], respectively. Thus, a strong discharge for addressing can be generated by lower address voltage in cases 2 and 3.

Figure 7 shows the IR intensity relative to the measured V_t closed-curve and discharge transient contour in Fig. 6. In case 1 of Fig. 7, the IR intensity is slowly increased by an increase in the applied voltage (V_a). However, in case 3, the IR intensity is dramatically increased. It is expected that the address discharge delay time can be improved.

Figure 8 and Table 4 show the address discharge delay time relative to the negative falling ramp voltage (V_{nf}). As shown in Fig. 8 and Table 4, with a decrease in V_{nf}, the statistical discharge time lag (T_s) decreases, but the formative discharge time lag (T_f) is almost the same. In case 3, as the V_{nf} decreases, T_f does not change, and Ts decreases by about 80 ns. The resultant total address discharge time lag ($T_d = T_f + T_s$) in case 3 decrease by about 85 ns. This result means that the smaller the portion of the wall voltage in the cell voltage is, the shorter the statistical discharge time lag is. In addition, it means that the wall voltage is set up to generate a fast address discharge by discharge between AY discharge and XY discharge in the microdischarge cell. Therefore, it is advantageous to use the electric field from the applied voltage during an address discharge instead of utilizing the wall charges from the reset period for stable and fast addressing.

Conclusions

The address discharge characteristics strongly depend on the wall charges that have been accumulated from reset period. The analysis of V_t closed-curve and monitoring of the corresponding IR emission show that the less amounts of wall charges prior to an address discharge induce the decrease of the statistical time lag and total address discharge time lag in an address period, resulting in a stable and fast addressing. To obtain a stable and fast address discharge, there is an advantage to use the electric field from the applied voltage than to use the wall voltage from reset period in address discharge.

Acknowledgment

This research was supported by Basic Science Research Program through the National Research Foundation of Korea (NRF) funded by the Ministry of Education (2013R1A1A4A03008577).

References

[1] Kim, J. Y., & Tae, H.-S. (2007). *IEEE Trans. Plasma Science*, *35*, 1766.
[2] Sakita, K., Takyama, K., Awamoto, K., & Hashimoto, Y. (2001). *IDW'01 Digest*, 841.
[3] Park, H.-D., Kim, J.-H., Tae, H.-S., Kim, D. M., & Seo, J. H. (2011). *SID'11 Digest*, 1468.
[4] Sakita, K., Takyama, K., Awamoto, K., & Hashimoto, Y. (2001). *SID'01 Digest*, 1022.
[5] Park, H. D., Kim, J. Y., & Tae, H.-S. (2007). *SID'07 Digest*, 569.
[6] Tae, H.-S., Jang, S.-K., Cho, K.-D., & Park, K.-H. (2006). *IEEE Trans. Electron Devices*, *53*, 196.